

Low creep and hysteresis silicon load cell based on a force-to-liquid pressure transformation

Robert A.F. Zwijze, Remco J. Wiegink, Theo S. J. Lammerink and Miko Elwenspoek
Mesa Research Institute, University of Twente, P.O.Box 217, 7500 AE Enschede,
The Netherlands

SUMMARY

Important problems in load cells are creep and hysteresis. Expensive high grade steels are used in order to reduce these effects. In this paper a silicon load cell design is presented which is based on a force-to-liquid-pressure transformation. The design is insensitive to hysteresis and creep, can be made at very low costs and is able to measure loads up to 1000 kg with an accuracy of 0.03 %. Analytical, numerical and experimental results on a macroscopic steel load cell are in very close agreement with each other.

Keywords: load cell, force measurement, creep, hysteresis

1 INTRODUCTION

Load cells are for example used in weighing bridges for lorries, cars and trailers. Also in industries where bulk material is worked up, it is necessary to measure masses as accurate as possible. Most current load cells are made of steel. The performance of these load cells is limited by hysteresis and creep even when expensive high grade steels are used.

The load cell we are aiming at has the following specifications and will be made of steel:

- maximum load: 10000 N (1000 kg)
- accuracy of full scale: 0.03 % = 0.3 kg
- temperature range: -10 up to 50 °C
- production costs: less than US \$ 75
- calibration: once in two years

The load cell discussed in this paper transforms the force into a liquid pressure which is enclosed in a bucket and locked up by a silicon membrane (figure 1). This pressure carries most part of the load. It is shown that the pressure difference between the liquid and the air is independent of creep and hysteresis in the silicon membrane. The pressure can be measured by a very small other membrane which is also in contact with the liquid. The theory for the calculation of the pressure is worked out in this paper. However, this requires the (complex) design of a small pressure sensor. Besides, we only want to test the mechanical structure. For these reasons the practical working out in this paper only focuses on the deformation of the membrane and the deflection of the boss.

In [2], a force-to-liquid-pressure load cell was introduced as a new kind of load cell. It consists of a piston under which the fluid is locked up by a seal. Characteristic for this kind of load cells is the high sensitivity. However, the load cell presented in [2] is rather sensitive to hysteresis. Another disadvantage is that it needs a standard Teflon seal which requires a proper surface finish of the mating steel parts. The load cell discussed in this paper does not have these drawbacks.

In section 2 the concept and process scheme of the load

cell is explained. Section 3 considers the analytical modeling of the load cell. The realisation and experiments on a macroscopic steel load cell are treated in section 4. The experiments are compared to analytical and finite element calculations. Finally, in section 5 some conclusions are drawn.

2 CONCEPT AND PROCESS SCHEME

Figure 1 shows a schematic drawing of the load cell which has a circular form. The liquid is locked up by the silicon membrane. The force which is applied to the boss of the silicon causes a downward deflection of this boss. The fluid under the boss is pressed outward and causes a deflection of the membrane. The silicon wafer is highly conductive and a displacement of the boss can easily be measured by measuring the capacitance change between the boss and a metal electrode beneath it. The deformation of the membrane can be measured by using platinum strain gauges. These gauges are not shown in figure 1.

The process scheme is indicated in figure 2. First of all three mask are made which define the three depths in the silicon. In the next step Reactive Ion Etching (RIE) is

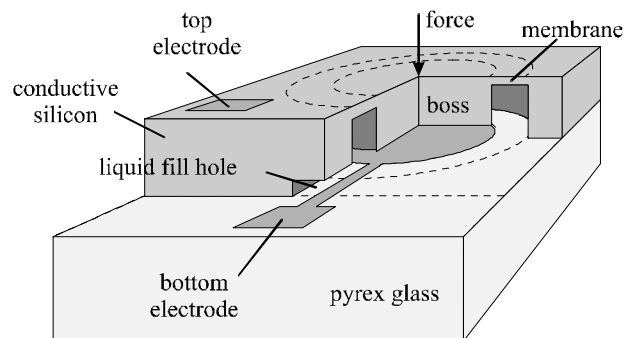


figure 1: Layout silicon load cell.

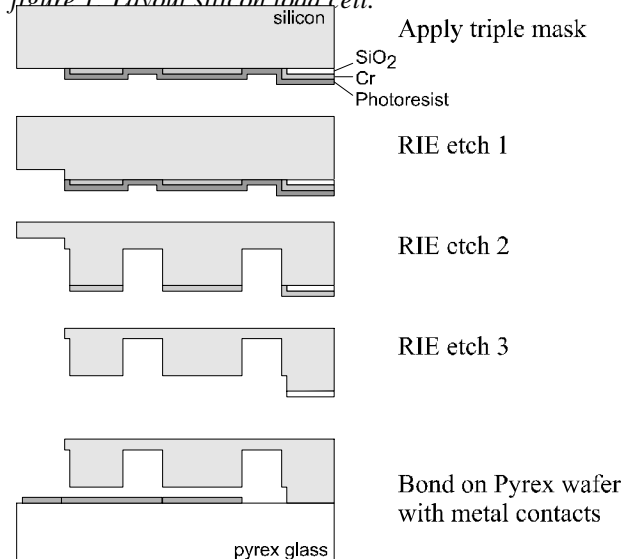


figure 2: Process scheme.

applied to the part of the silicon which has to be etched through. Then, the photoresist is removed and the silicon under the membrane is etched. After removal of the Chromium mask the silicon under the boss and the fill hole for the liquid is etched. The Pyrex glass wafer only needs to be covered with an aluminum layer which defines the bottom electrode. The next production step is the anodic bonding of both wafers. The last step is the filling with liquid. This is done by placing the load cell in a liquid which in turn is placed in vacuum clock. Then, the pressure must be decreased to a value close to the vapor pressure of the liquid. Now, when the load cell has two filling holes, it is automatically filled. The holes are closed with glue. The filling process has been tested with success. However, a complete silicon load cell has not yet been realized.

3 ANALYTICAL MODELING

In this section the load cell is modeled mathematically. In §3.1 it is assumed that the water is incompressible. Under this assumption, the pressure-force relation, deformation profile of the membrane and the stresses in the membrane are calculated. Then, in §3.2 the influence of compressibility of the liquid is taken into account. Finally, in §3.3 temperature effects are considered.

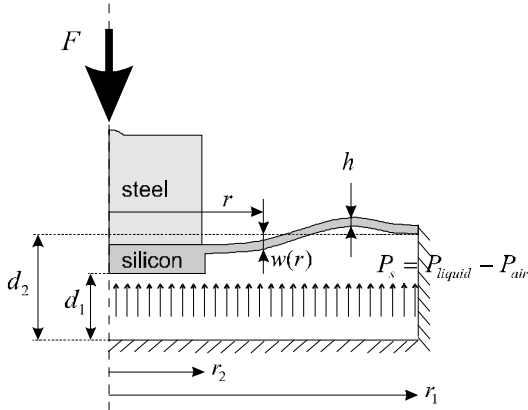


figure 3: Deformation of membrane and boss.

3.1 Incompressible fluid

In figure 3 the deformation of the membrane and the deflection of the boss for some load F is shown. The pressure-force ($P_s - F$) relation and deflection profile of the membrane are derived in the next way:

- Use classical plate elasticity theory [1].
- The deflection profile $w(r)$ of the membrane has to satisfy some boundary conditions:

$$w(r = r_1) = \frac{dw}{dr}(r = r_1) = \frac{dw}{dr}(r = r_2) = 0. \quad (1)$$

- Incompressibility of the fluid is satisfied if the following condition is fulfilled:

$$Pr_2^2 w(r = r_2) + \int_{r=r_2}^{r_1} 2Pr w(r) dr = 0. \quad (2)$$

Now, the expression for the deflection $w(r)$ of the membrane can be derived:

$$w(r) = \frac{F(n^2 - 1)}{PEh^3} I\left(\frac{r_1}{r_2}, r_1, r\right). \quad (3)$$

n is Poissons ratio, E Youngs modulus of silicon and h the thickness of the membrane. $I(r_1/r_2, r_1, r)$ is a rather complex function. An impression of the deformation of the membrane for some chosen parameters is given in figure 4. The values of these parameters will be explained in §3.3.

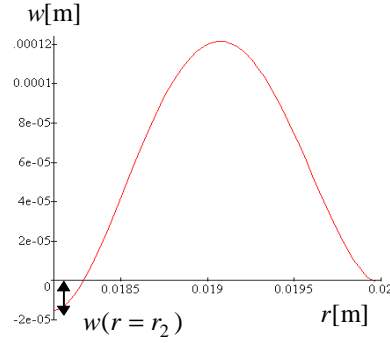


figure 4: Deformation of the membrane ($F = 10000 \text{ N}$, $E = 150 \text{ Gpa}$, $n = 0.25$, $h = 55 \text{ mm}$, $r_1 = 20 \text{ mm}$, $r_2 = 18.116 \text{ mm}$, $d_1 = 16 \text{ mm}$, $d_2 = 325 \text{ mm}$).

The pressure-force relation follows from (2):

$$P_s = \frac{F}{A_{eff}}, \quad A_{eff} = \quad (4)$$

$$\frac{Pr_2^2}{P} \frac{(1 - 4s^2 + 6s^4 - 4s^6 + s^8)}{(3.82 \ln(s)[s^2 - s^4] + 0.95[1 - s^2 - s^4 + s^6])}, \quad s = \frac{r_1}{r_2}.$$

A_{eff} is called the effective area. Equation (4) shows that there is no dependence on Youngs modulus of the silicon membrane so that it is concluded that the pressure is insensitive to hysteresis and creep in the membrane. Although the deflection of the silicon boss and the deformation profile of the membrane do depend on the Youngs modulus of silicon, they are not expected to change much during loading. The reason for this is that silicon, because of its mono crystalline structure, hardly shows any hysteresis and creep. An impression of the effective area in comparison to the total area of the bucket (=area of boss + membrane) and the boss is shown in figure 5. From this figure it can be concluded that the effective area lies somewhere between the area of the boss and the bucket. For the parameters given in the caption of figure 4 the pressure sensitivity is calculated from (4) giving $\frac{\partial P_s}{\partial F} = 875.96 \text{ Pa} / \text{N}$.

As the membrane is rather thin it must be checked whether the critical stress is not exceeded. In the

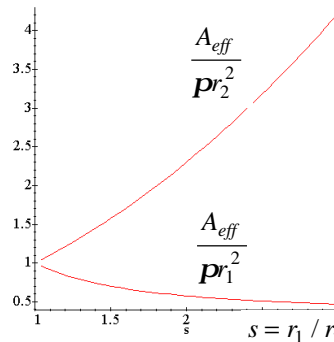


figure 5: Effective area divided by the area of the bucket and effective area divided by the area of the boss as a function of the ratio r_1 / r_2 .

membrane three stresses are present: radial, tangential stress and shear stress which is acting in the direction of force F (\mathbf{s}_r , \mathbf{s}_t and \mathbf{t} respectively). The first two are calculated from their corresponding moments [1] and they have a maximum on the top and bottom sides of the membrane. As all three stresses occur at the same place in the membrane, the Von Mises stress criterion is used for comparison to the maximum allowable stress. It is given by

$$\mathbf{s}_V = \sqrt{\frac{1}{2}[(\mathbf{s}_r - \mathbf{s}_t)^2 + \mathbf{s}_t^2 + \mathbf{s}_r^2 + 6\mathbf{t}^2]} \quad (5)$$

A plot of all the stresses is shown in figure 6. The ultimate stress of silicon is about 7 Gpa [3], so it should be possible to bear a load of 10000 N.

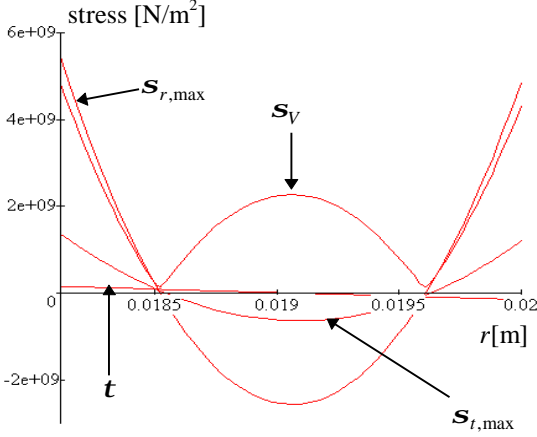


figure 6: Radial, tangential, shear and Von Mises stresses in the silicon membrane.

As the shear stress \mathbf{t} is very small in comparison to $\mathbf{s}_{r,\max}$ and $\mathbf{s}_{t,\max}$ this stress can be neglected. Besides, it is seen that the maximum stresses occur at $r = r_2$. Therefore, the maximum Von Mises stress in the membrane is approximately given by

$$\mathbf{s}_{V,\max} = \frac{3F\sqrt{(1-n-n^2)}}{4ph^2} \mathbf{g}(s), \quad (6)$$

$$\mathbf{g}(s) = \frac{(4\ln(s)s^4 - 5s^4 + 8\ln(s)s^2 + 4s^2 + 1)}{(1-2s^2 + s^4)}$$

The function $\mathbf{g}(s)$ is drawn in figure 7. It is concluded that the maximum stress strongly depends on the thickness h of the membrane. The dependence on the ratio r_1/r_2 is less strong.

3.2 Compressible fluid

By including compressibility of the fluid, equation (2) is changed to

$$pr_2^2 w(r=r_2) + \int_{r=r_2}^{r_1} 2pr w dr = \Delta V = V_0 \frac{P_s}{E_v}, \quad (7)$$

where E_v is the bulk compressibility modulus of the liquid, V_0 the initial volume and ΔV the decrease in volume of the compressed fluid. For water $E_v = 2.24 \text{ GN/m}^2$. The effective area is calculated in the same way as done in §3.1 giving

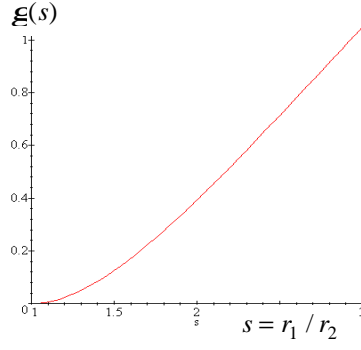


figure 7: Von Mises stress parameter $\mathbf{g}(s)$.

$$A_{\text{eff}} = P_2^2 \frac{\left\{ 1 - 3s^2 + 3s^4 - s^6 + \frac{16V_0 E h^3}{p E_v r_1^6 (n^2 - 1)} s^6 \right\}}{3.82 \ln(s)s^2 + 0.95[1 - s^4]} \quad (8)$$

As, in the term $\frac{16V_0 E h^3}{p E_v r_1^6 (n^2 - 1)}$ Youngs modulus appears,

it must be chosen as small as possible. The most simple tool for reducing this term is by giving a very small value to the initial volume of the liquid. For the parameters given in the caption of figure 4 the pressure-sensitivity now equals $\mathcal{P}_s / \mathcal{F} = 875.90 \text{ [Pa/N]}$ which only deviates 0.0007 % from the incompressible case. So it is concluded that the condition of incompressibility can be maintained.

3.3 Dependence on temperature

The effective area on which the liquid presses, changes linearly with temperature:

$$\frac{dA_{\text{eff}}}{dT} = 2\mathbf{a}_{\text{silicon}} A_{\text{eff}} \quad (9)$$

T is the temperature and $\mathbf{a}_{\text{silicon}}$ the temperature expansion coefficient of silicon. However, due to large differences in temperature expansion coefficients of the silicon and liquid, this overrules the change in effective area. Practical values are $\mathbf{a}_{\text{silicon}} = 2.33 \cdot 10^{-6} \text{ }^\circ\text{C}^{-1}$ and for water at 20 °C, $\mathbf{a}_{\text{water}} = 207 \cdot 10^{-6} \text{ }^\circ\text{C}^{-1}$. In order to model this effect, (2) is changed to

$$pr_2^2 w(r=r_2) + \int_{r=r_2}^{r_1} 2pr w(r) dr = -V_0 3(\mathbf{a}_{\text{liquid}} - \mathbf{a}_{\text{silicon}}) \Delta T. \quad (10)$$

By putting F equal to zero it is calculated from (10) that the pressure-temperature sensitivity is given by

$$\frac{dP_s}{dT} = 15.29 \frac{s^6 h^3 E (\mathbf{a}_{\text{liquid}} - \mathbf{a}_{\text{silicon}}) V_0}{(1-n^2) r_1^6 (s^6 - 3s^4 + 3s^2 - 1)} \quad (11)$$

The pressure variation (error) which is introduced by temperature variations must always be considered with respect to the pressure at full load (that is 10000 N). Therefore, in minimising the temperature error, one has to minimise

$$\text{error} = \left(\Delta T_{\max} \frac{dP_s}{dT} \right) / \left(F_{\max} \frac{dP_s}{dF} \right) \quad (12)$$

Substitution of (4) and (11) in (12) gives

$$error = \frac{16\Delta T_{\max} V_0 (\mathbf{a}_{liquid} - \mathbf{a}_{silicon}) E h^3}{F_{\max} r_1^4} \mathbf{k}(s, \mathbf{n}),$$

$$\mathbf{k}(s, \mathbf{n}) = \frac{s^4}{\left((1 - \mathbf{n}^2) s^4 - (1 - \mathbf{n}^2) \ln(s) s^2 - 1 + \mathbf{u}^2 \right)}. \quad (13)$$

So, it can be concluded that the liquid volume and Youngs modulus must be decreased and that both thermal expansion coefficients must match as close as possible. It could also be concluded that h must be decreased, r_1 increased and s increased. However, one has to take into account that the change of these parameters leads to a change in the maximum Von Mises stress (see (6)). So, one has to incorporate the maximum Von Mises stress in (13). $\mathbf{s}_{V, \max}$ is introduced into (13) by solving h from (6), resulting in

$$error = \frac{\Delta T_{\max} \sqrt{F_{\max}} V_0 (\mathbf{a}_{liquid} - \mathbf{a}_{silicon}) E}{\mathbf{s}_{V, \max}^{1.5} r_1^4} \mathbf{b}(s, \mathbf{n}). \quad (14)$$

The function $\mathbf{b}(s, \mathbf{n} = 0.25)$ is plotted in figure 8. It is concluded that $s = r_1 / r_2$ should be chosen as small and r_1 as large as possible. Now, by using (14) and putting $\mathbf{s}_{V, \max} = 5$ GPa, an error of 0.03 % is calculated for the parameters in the caption of figure 4. This means that the silicon load cell needs no temperature correction.

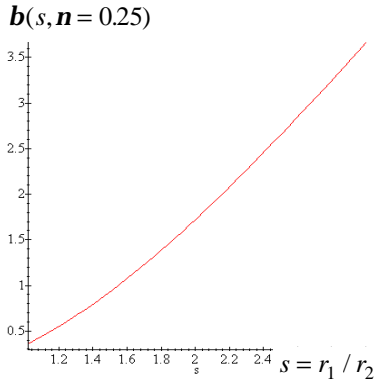


figure 8: Error parameter $\mathbf{b}(s, \mathbf{n} = 0.25)$.

4 MACROSCOPIC STEEL LOAD CELL

In order to test the theory a macroscopic load cell of steel has been made (see figure 9). The pressure was measured with a commercial Honeywell silicon pressure sensor. Hysteresis of the load cell was tested by loading, then unloading and hereafter loading the load cell with some weight. The output of the Wheatstone bridge of the pressure sensor is shown in figure 10. The two measurements that were done for each point cannot be distinguished in the figure. The load cell behaves linearly and the experimental pressure sensitivity equals $(\mathcal{P}_s / \mathcal{F})_{\text{exp}} = 249$ Pa / N which is in very close agreement with the analytical result $(\mathcal{P}_s / \mathcal{F})_{\text{ana}} = 250.03$ Pa / N. The hysteresis as a percentage of the output at maximum load is less than 0.009 % which is far more accurate than the 0.03 % that was specified in section 1. The load cell is also analyzed with the finite element program Ansys 5.3. For the (compressible) fluid, FLUID79 elements are taken. Ansys

predicts a sensitivity of $(\mathcal{P}_s / \mathcal{F})_{\text{Ans}} = 247.05$ Pa / N which is in very good agreement with the experimental and analytical results.

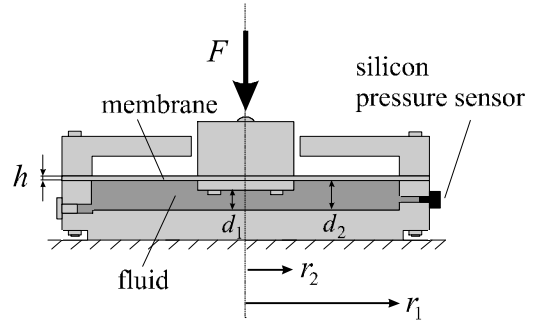


figure 9: Layout macroscopic steel load cell $E = 210$ Gpa, $\mathbf{n} = 0.3$ $h = 1$ mm, $r_1 = 5$ cm, $r_2 = 2$ cm, $d_1 = 5$ mm and $d_2 = 10$ mm).

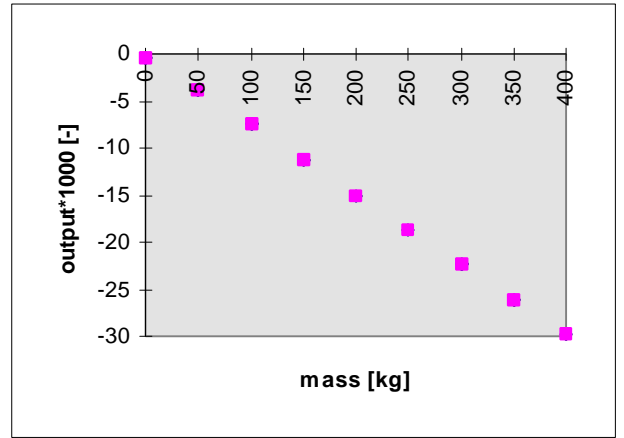


figure 10: Pressure sensor output of the macroscopic steel load cell.

5 CONCLUSIONS

The design and modelling of a silicon force-to-liquid pressure load cell has been described. It is proved that the force-pressure relation is independent of the Youngs modulus of the membrane and therefore is independent of hysteresis and creep. The analytical, numerical and experimental results of a macroscopic steel model are in very close agreement with each other so that the theory is correct. This model shows a hysteresis error of less than 0.009 %. The filling of small cavities for the silicon model has been tested. The silicon load cell needs no temperature correction, because this error is maximal 0.03 %. The silicon load cell will be realised in the future.

ACKNOWLEDGEMENTS

This research is supported by the Dutch Technology Foundation (STW).

REFERENCES

- [1] S.P. Timoshenko and S.W. Woinowsky-Krieger, Theory of plates and shells, McGraw-Hill International Editions, Singapore, 1959.
- [2] H. Kazerooni, M.S. Evans and J. Jones, Hydrostatic force sensor for robotic applications, Journal of dynamic systems, measurement and control, 119(Issue 1), 1997, 115-119.
- [3] Peterson, K.E., Silicon as a mechanical material, Proceedings of the IEEE, 70(1982), 420-457.